# Development and implementation of multicomponent liquid wall film evaporation model for internal combustion engine applications

**Baleta, Jakov; Vujanović, Milan; Melo, Rui**

*Source / Izvornik:* **The Holistic Approach to Environment, 2017, 7, 15 - 27**

**Journal article, Published version**
**Rad u časopisu, Objavljena verzija rada (izdavačev PDF)**

*Permanent link / Trajna poveznica:* https://urn.nsk.hr/urn:nbn:hr:115:091998

ISSN 1848-0071
621.43+622.75=111
Recieved: 2016-08-30
Accepted: 2016-10-27
Original scientific paper

# DEVELOPMENT AND IMPLEMENTATION OF MULTICOMPONENT LIQUID WALL FILM EVAPORATION MODEL FOR INTERNAL COMBUSTION ENGINE APPLICATIONS

**JAKOV BALETA, MILAN VUJANOVIĆ, RUI MELO[1]**

Faculty of Mechanical Engineering and Naval Architecture, University of Zagreb, Croatia
[1]TORBEL – Torres & Belo, S.A., Zona Industrial Ervosas Ílhavo, Portugal
e-mail: jakov.baleta@fsb.hr

Various environmental regulations put ever stringent requirements on the automotive industry as a part of solution to the problem of global warming and climate change. Engine emissions are influenced, among others, also with quality of fuel and air mixing process. Auto ignitability of fuel in cylinder depends on detailed chemical composition of the fuel as well as on the evolution of the thermal and compositional state of the fuel mixture. The evaporation of wall film, formed by spray/wall impingement has strong effects on engine emission. This works aims at further development of the numerical model of liquid wall film by implementation and validation of mathematical models of multicomponent wall film evaporation. Two multicomponent liquid film evaporation models were developed, the first one on the basis of analogy between momentum and mass transfer, and the second one employing modified wall functions which take into account influence of the evaporation on boundary layer above liquid film. Particular scientific contribution is in implementation of the UNIFAC method for activity coefficients calculation. Finally, implemented models were compared with available experimental data in order to confirm their validity.
**Key words:** computational fluid dynamics, multicomponent evaporation, turbulent boundary layer, UNIFAC method, wall function, wall film.

**Razvoj i implementacija modela višekomponentnog isparavanja filma kapljevine na stjenci za primjenu u motorima s unutrašnjim izgaranjem.** Različiti propisi za zaštitu okoliša nameću sve strože zahtjeve na sektor automobilske industrije kao dio rješenja za problem globalnog zatopljenja i klimatskih promjena. Emisije iz motora su uzrokovane, između ostaloga, također i kvalitetom procesa miješanja gorivih para i zraka. Autozapaljenje goriva u cilindru ovisi o detaljnom kemijskom sastavu goriva, kao i o evoluciji termičkog i kemijskog sastava gorive smjese. Isparavanje filma kapljevine na stjenci formiranog uslijed udaranja kapljica spreja u stjenku ima snažan utjecaj na emisije motora. Ovaj rad usmjeren je na daljnji razvoj numeričkog modela filma kapljevine na stjenci kroz implementaciju i validaciju matematičkih modela višekomponentnog isparavanja filma. Razvijena su dva modela višekomponentnog isparavanja filma; prvi na bazi analogije između prijenosa količine gibanje i mase, a drugi koristeći modificirane zidne funkcije koje uzimaju u obzir utjecaj isparavanja na granični sloj iznad filma kapljevine. Konačno, implementirani modeli su uspoređeni s dostupnim eksperimentalnim podacima s ciljem potvrđivanja njihove ispravnosti.
**Ključne riječi**: računalna dinamika fluida, višekomponentno isparavanje, turbulentni granični sloj, UNIFAC metoda, zidna funkcija, film kapljevine na stjenci.

## INTRODUCTION

Liquid film flow sheared by an external air flow field is a physical phenomenon encountered in many engineering applications such as: burners, rain on vehicle windows and aircraft wings, rocket nozzles, mist eliminators, heat exchangers, steam turbine blades and especially internal combustion (IC) engines, where its proper description is important condition in order to comply with stringent environmental regulations. In IC engines it has been observed that unburned fuel that goes

directly into the manifold causes an increase in the emissions of unburned hydrocarbons in the petrol engines and larger product of soot in the compression-ignited engines, especially under cold start conditions. The quality of mixing between gas phase and liquid film vapour is crucial for efficient operation of chemical reactors utilizing favourable mass and heat transfer characteristics of liquid film. Above mentioned examples show great importance of the correct prediction of wall film behaviour.

Multicomponent evaporation modelling approach can be generally divided into two model groups: discrete multicomponent models and continuous multicomponent models [1]. Discrete multicomponent evaporation models track individual fuel components and enable direct coupling of reaction kinetics to the individual fuel components, whilst continuous multicomponent models are based on the continuous thermodynamic method and describe fuel composition as continuous distributed function with respect to some parameter, such as the molecular weight [2]. The latter approach decreases computational demands compared to the former one, but tends to be inaccurate if detailed chemical calculations are needed, or in the case of mixtures composed of large number of components. As current demands for computational simulation accuracy are relatively high, this section will only deal with discrete multicomponent evaporation models. O'Rourke and Amsden [3] showed that the evaporation affects structure of the turbulent boundary layer near the wall due to perpendicular velocity component of evaporated chemical species. In order to properly describe this effect, they have derived provisional wall functions that inhibit transport and reduce to standard ones in the case of walls without the wall film. Zeng and Lee [4] have suggested the model for multicomponent liquid wall film evaporation that is basically generalization of the model of O'Rourke and Amsden to more components. In their work they modeled film concentrations and temperature non-uniformity by employing third order polynomial. Torres and al. [5] took this approach one step further by discretizing liquid film. That way, a higher calculation accuracy is achieved, but at the expense of calculation time. Ebrahimian [6] has developed the most accurate model of liquid film evaporation which, like approach in [4], employs third order polynomial for film temperature distribution. However, it also takes into account the chemical species enthalpy diffusion, Stefan flow and generalizes wall functions, developed on the basis of the direct numerical simulation [7], on the multicomponent evaporation case. In spite of all the advantages of this model, its validation is still missing.

An alternative approach is also possible by employing volume of fluid (VOF) method. However, this approach is suitable only for some rather specific investigation cases. For example Cui et al. [8] investigated heat and mass transfer of a multicomponent two-phase film flow in an inclined channel at sub-atmospheric pressure. Simulation was performed on simple 2-D axisymmetric domain. Haelssig et al. [9] performed direct numerical simulation of interphase heat and mass transfer in multicomponent vapour–liquid flows on the geometry of a 2-D channel having a width of 6 mm and a length of 30 mm. Due to high computational demands simulations described in [8] and [9] are used for parameter analysis and obtaining more profound knowledge of basic physical phenomena, and cannot be used for performing real engineering devices simulations within reasonable time. Finally, the most recent approach for treating liquid film evaporation is by employing some analytical expressions after suitable simplification of governing differential equations is performed. Liye et al. [10]

proposed a new approach to modelling transient heating in evaporating fuel film, with energy governing equation solved analytically. This work, however, doesn't deal with multicomponent evaporation. The results from Liye et al. [10] were basis for verification of the similar analytical model from Yan et al. [11] which also analysed only single component evaporating liquid films. The results from parametric analysis have shown that the evolution behaviour of the wall film evaporation can be divided into three stages as follows; initial rapid heating, slow heating and final rapid heating stage.

Taking into account all stated, the goal of this paper is additional improvement of the Eulerian liquid wall film model through development and implementation of two multicomponent liquid film evaporation models, the first one on the basis of analogy between momentum and mass transfer, and the second one employing modified wall functions which take into account influence of the evaporation on boundary layer above liquid film. Particular scientific contribution is in implementation of the UNIFAC method for activity coefficients calculation, which is employed for the first time in the area of liquid wall films. The rest of the paper is organized as follows; after presenting relevant mathematical models that are the basis of wall film numerical representation and part of the newly developed model, experimental setup taken from literature for validation purposes is given. Afterwards, results of the conducted simulation study are discussed and conclusions are derived together with the recommendation for the future work.

## MATHEMATICAL MODEL

Many multi-dimensional numerical models of single-component liquid film have been developed in the past. Models developed by O'Rourke and Amsden [3] and Desoutter [12] adopt a Lagrangian particle tracking method, whereas the models of Stanton and Rutland [13], Bai and Gosman [14], Foucart et al. [15], Wittig [16], Lucchini et al. [17] and Cazzoli and Forte [18] describe the dynamics of the liquid film by an Eulerian approach.

Commercial computational fluid dynamics (CFD) code AVL Fire employed during the research conducted in this work is based on the Eulerian approach and this section will present its mathematical structure of, both existing and newly implemented models.

It is necessary to employ thin film assumption, valid for films with thickness in the range of ≈100 μm, since a 3D two phase flow simulation of liquid wall film is currently too demandable from computational point of view. By integrating across the film thickness, the liquid film can be represented as a two dimensional flow over three dimensional surface, i.e. continuity equation is transformed in the equation for film thickness conservation:

$$\frac{\partial \delta}{\partial t} + \frac{\partial \delta u_1}{\partial x_1} + \frac{\partial \delta u_2}{\partial x_2} = \frac{1}{\rho A}(S_{mD} - S_{mV}) \qquad (1)$$

where $\delta$ represents film thickness, $u_1$ and $u_2$ are film velocity components, $A$ is surface area of film patch and $S_{mD}$ represents film mass source due to liquid introduction by feeder, spray droplets impingement and condensation, whilst $S_{mV}$ represents sink terms of film mass as a consequence of film rupturing, evaporation and entrainment. It can be seen that the form of equation (1) allows us to describe liquid film without the need for computational grid adjustment in its vicinity.

Film velocity components could be calculated by imposing assumed velocity profile depending upon whether film flow regime is either laminar or turbulent, or they

can be obtained by solving momentum equation in the form:

$$\frac{dM_i}{dt} = \oint_L \rho\delta u_i (u_i - V_j)\hat{n}_i dL + \oint_L p\delta\hat{n}_i dL + mg_i + \Gamma_i + S_M \quad (2)$$

where $M_i$ is film momentum, $\rho$ is the film density, $u_i$ is film velocity, $V_j$ is wall velocity, $\hat{n}_i$ is normal to the face cell facing outwards, $L$ is length of the face cell boundary, $\delta$ is film thickness, $p$ is film pressure, $m$ is film mass, $g_i$ is gravity vector, $\Gamma_i$ is the term that takes into account all shear stresses and $S_M$ presents various source and sink terms, such as film entrainment, spray droplets impingement and film evaporation.

In the Fire the default approach for liquid film temperature is to take the same value as the wall underneath. This is valid only for very thin films, and to provide a more appropriate treatment the energy balance for the film can be solved. For this purpose a homogeneous mean film temperature is calculated using a lumped parameter equation in each film cell. This equation takes into account the following sources [19]:

- conductive heat transfer between film and wall and between film and gas phase flow;
- convective heat transfer within the film;
- enthalpy transfer from spray droplet impingement;
- enthalpy loss from droplet entrainment;
- enthalpy transfer via latent heat during evaporation.

The enthalpy balance equation can be written as:

$$\frac{\partial\rho\delta h}{\partial t} + \frac{\partial h\delta u_1}{\partial x_1} + \frac{\partial h\delta u_2}{\partial x_2} = \frac{1}{A}\left(\dot{H}_{sor,wf} - \dot{H}_{sor,fg} - \dot{m}_{ev}h_{ev} + \dot{H}_{sor,im} + \dot{H}_{sor,ent}\right) \quad (3)$$

where $h$ is film specific enthalpy, $\dot{H}_{sor,wf}$ is heat flux from wall side, $\dot{H}_{sor,fg}$ is heat flux from the gas phase boundary layer above the film, $\dot{m}_{ev}$ liquid film evaporation rate, $h_{ev}$ is enthalpy of evaporation, $\dot{H}_{sor,im}$ is energy flux from impacting spray droplets and $\dot{H}_{sor,ent}$ energy flux leaving the film due to film entrainment. The enthalpy transport equation (3) is solved in the semi-implicit way due to numeric stability, using a subcycling procedure with upwinding for the convective fluxes [19].

Finally, species conservation equation could be represented similar to enthalpy transport equation (3):

$$\frac{\partial\rho\delta\gamma_i}{\partial t} + \frac{\partial\gamma_i\delta u_1}{\partial x_1} + \frac{\partial\gamma_i\delta u_2}{\partial x_2} = \frac{1}{A}\left(S_{\gamma i,D} - S_{\gamma i,V}\right) \quad (4)$$

In the expression above $\gamma_i$ represents concentration of $i$-th liquid component in the film mixture, $S_{\gamma i,D}$ represents source of $i$-th liquid film component due to introduction by feeder, spray droplets impingement and condensation, whilst $S_{\gamma i,V}$ represents sink terms for $i$-th liquid film component as a consequence of evaporation. The species transport equation (4) is solved in the same way as enthalpy transport equation.

As mentioned previously, by using resemblance between momentum and mass transfer, the dimensionless Stanton number for mass transfer is introduced:

$$St_{m,i} = \frac{\eta c_f}{Sc_t(1 + P_m\sqrt{\eta c_f})} \quad (5)$$

where $Sc_t$ represents turbulent Schmidt number fixed to 0.9, $c_f$ is local friction factor, $P_m$ is correction factor which takes into account the influence of the laminar sublayer on the mass transfer on rough surfaces and $\eta$ is correction factor for film waviness.

Local friction factor $c_f$ is implementing the analogy to momentum transfer by directly using logarithmic law of the wall:

$$c_f = \frac{\tau_w}{\rho u_{//}^2} = \left[\frac{1}{\kappa}\ln\left(Ey^+\right)\right]^{-2} \qquad (6)$$

In the above expression $\tau_w$ is shear stress and $u_{//}$ is film parallel velocity.

The aforementioned correlation $\eta$ was developed by Burck [20] and extended by Sill [21] for evaporating water films. This correlation was developed originally for heat transfer and it can be written in the following form to describe mass transfer enhancement:

$$\eta = \log\frac{\mathrm{Pr}^{0.33}}{\mathrm{Re}_{ks}^{0.243}} - 0.32\cdot 10^{-3} \qquad (7)$$

$$\mathrm{Re}_{ks}\log(Sc) + 1.225$$

Finally, $P_m$ was developed by Jayatilleke [22] with the goal to encompass resistance of laminar sub-layer to momentum and heat transfer. Again, this correlation should be modified for mass transfer resistance:

$$P_m = 9.0\left(\frac{Sc}{Sc_t} - 1\right)\left(\frac{Sc_t}{Sc}\right)^{0.25} \qquad (8)$$

Liquid film evaporation rate of each component can be written using the modified Stanton number as:

$$\dot{m}_i = -\rho_v u_{//}\frac{St_{m,i}}{\beta_{stefan,i}}\frac{c_i - c_{i,s}}{1 - c_{i,s}} \qquad (9)$$

where $\rho_v$ represents vapour density and $c_i$ is concentration of the liquid film component in the gas phase above the film.

Stefan flux correction is defined as:

$$\beta_{stefan,i} = \frac{\ln\left\{\left[p - p_i(y)\right]/\left(p - p_{i,s}\right)\right\}}{\left[p_i(y) - p_{i,s}\right]/\left(p - p_{i,s}\right)} \qquad (10)$$

where $p$ is static pressure of gas phase above the film, $p_i$(y) is partial pressure of $i$–th liquid component in the gas phase and $p_{i,s}$ is partial pressure of the $i$–th liquid component on the film/gas interface.

The heat transfer from the gas boundary layer was not modelled, but rather it was assumed the fixed value of Nusselt number equal to 2. This assumption was proved to be sound for many practical cases by the experimental tests carried out by AVL.

As has been previously stated, there is also the other way for mathematical description of liquid film evaporation by employing wall functions. O'Rourke and Amsden were the first proponents of this approach. Liquid vaporization of wall film alters the structure of the turbulent boundary layer above the film due to gas velocity normal to the wall induced by the evaporation [3]. They derived provisional wall functions that inhibit transport of physical quantities above the vaporizing films and that reduce to standard wall functions [23] in case of non-vaporizing walls. These wall functions were generalized by Torres et al. [5]:

$$H_{Y,i} = \begin{cases} \dfrac{\rho C_\mu^{\frac{1}{4}} K^{\frac{1}{2}}}{y_C^+ Sc_{L,i} + (Sc_T/\kappa)\ln(y^+/y_C^+)}, & y^+ > y_C^+ \\ \dfrac{\rho C_\mu^{\frac{1}{4}} K^{\frac{1}{2}}}{y_C^+ Sc_{L,i}}, & y^+ \le y_C^+ \end{cases} \qquad (11)$$

The threshold value of $y_C^+ = 11.05$ is used to assess whether laminar or turbulent transport/boundary layer will take its place:

$$y^+ = \rho_L C_\mu^{\frac{1}{4}} K^{\frac{1}{2}} y/\mu_L, \qquad (12)$$

$y^+$ is wall normal distance, $C_\mu$ is constant equal to0.09, $K$ is turbulent kinetic energy and $\mu_L$ is laminar viscosity. The evaporation rate is calculated using Spalding number together with wall functions and concentration difference:

$$\dot{m}_i = -H_{\gamma,i}\frac{\ln(1+B)}{B}(c_i - c_{i,s}) \qquad (13)$$

Spalding number is defined as:

$$B = \frac{\sum_i c_{i,s} - \sum_i c_i}{1 - \sum_i c_{i,s}} \qquad (14)$$

As can be deduced by observing presented equations, concentration of vapour phase on the gas/liquid interface plays an important role for the accurate calculation of species vaporization rate. According to the insight given from available literature, most of the authors use saturation pressure of each liquid composing the film. Here is very important physical phenomena neglected – how each component influences the rest of the components in the mixture depending on its molecular structure. In order to describe this influence, activity coefficients were calculated using the UNIFAC method [24]. When considering the molecular interactions, the liquid mixture is assumed as a solution of the structural units of the molecules, rather on the sole molecules. The model relies on a data for the molecular behaviour of the investigated components [25]. UNIFAC method was implemented within this paper, and on the basis of studied literature, it can be stated that such an approach wasn't employed yet in the area of liquid wall films.

## EXPERIMENTAL CONFIGURATION

The test section presented on Figure 1 has a primary cross section of 83x60 mm and has been characterized with the turbulent intensity and an integral length scale of 5% [26]. The channel is divided with the film plate on two equal parts, each having height of 3.9 mm. The liquid film is introduced by feeder composed of a row of 0.5 mm holes, which are 0.8 mm apart. The test section provides six measurement planes, 80 mm apart. The first plane is 20 mm downstream from the start of the film plate and marks the starting point of the computational domain.

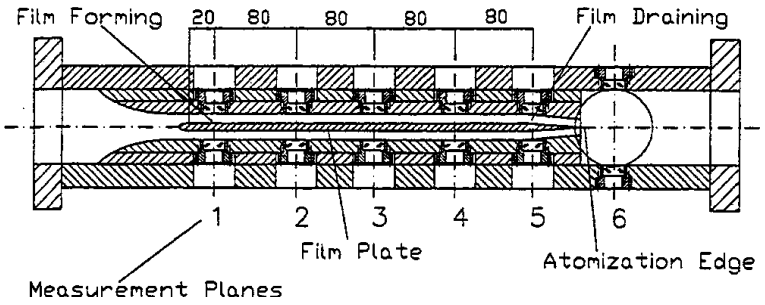


**Figure 1.** Schematic representation of the test section [27]
**Slika 1.** Shematski prikaz testne sekcije

The vapour concentration profiles are measured by taking gas samples through a probe and cooling them down in a condenser to 273 K. The vapour concentration in the gas phase of the condenser is calculated based on the condensate compound and the measured pressure and temperature in the condenser. The ratio of the mass flow rate of each component and the dry air represents the mass concentration of the vapour component at the probe tip [27].

## NUMERICAL SIMULATION SETTINGS

In order to reduce computational demands to acceptable level, only part of the domain was simulated. This was possible since flow within the channel has intrinsically symmetrical behaviour. Thus, only 5 mm of the channel width was simulated. The Figure 2 shows computational domain 300x5x3.9 mm with boundary conditions details. It consists of 15 000 control volumes.

Two cases were simulated with the goal of investigating the influence of gas phase pressure above the liquid film.

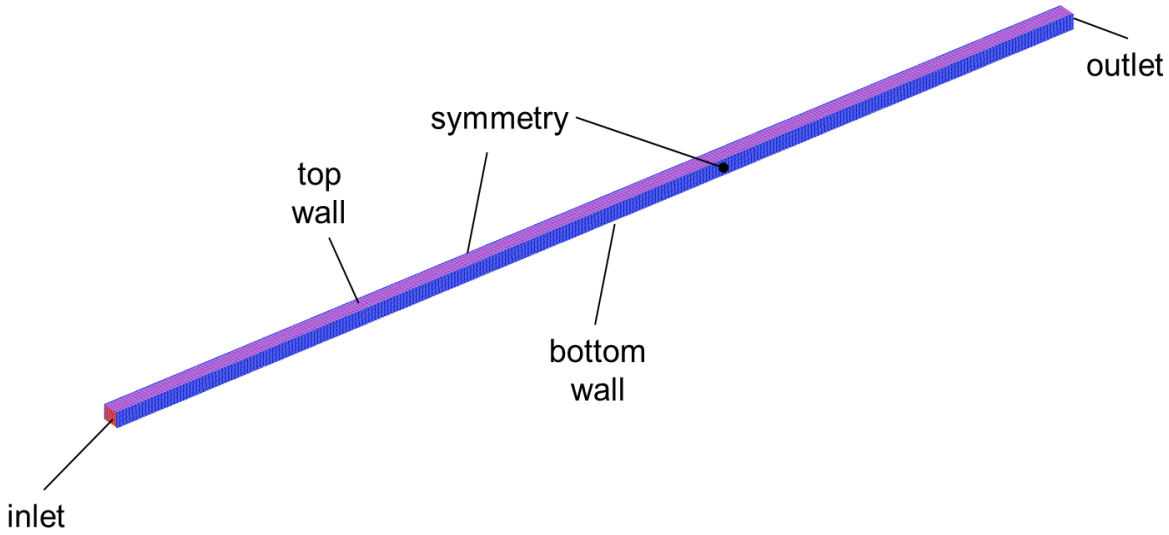


**Figure 2.** Mesh representation of the computational domain
**Slika 2.** Prikaz mreže računalne domene

Time step was 5e-04 s for all simulated cases in order to have stable calculations with criterion of Courant number <1. The adiabatic boundary condition was imposed on the top and bottom walls, whilst the symmetry boundary condition was set on the domain sides. Pressure on the outlet was either 1.1 or 2.6 bar, depending on the simulation case. For the turbulence, scalar and energy transport equations a first order UPWIND differencing scheme was applied, whilst for the continuity equation the central differencing scheme (CDS) was employed. The CDS can generate numerical oscillations yielding unbounded and non-monotonic solutions. Therefore, for the momentum equation a combination of MINMOD relaxed and UPWIND was proposed by introducing the blending factor of 0.5. The solution convergence criterion is achieved when the momentum, pressure and energy residuals decrease 4 orders of magnitude compared to the first iteration. The pressure velocity coupling of the momentum and continuity equation was obtained using the SIMPLE/PISO algorithm. Liquid, with equal mass fractions of ethanol and water, was introduced into the computational domain by means of feeder cell with mass flow rate of 1.5e-04 kg/s. Finally, turbulence quantities on the inlet were 5% for turbulent intensity and turbulent length scale and turbulence was modelled using $k$-$\varepsilon$ model.

## RESULTS AND DISCUSSION

First, the qualitative comparison between two multicomponent evaporation models in the central cross section is presented in the Figure 3. Since the O'Rourke modelling approach has approximately one order of magnitude lower concentration than the Wittig model, each model is presented with its own colour scale. Otherwise, gradients in the O'Rourke model wouldn't be visible. Relative change in water concentration in both measurement planes is similar, making the conclusion that both models describe similar relative dynamics of evaporation. However, O'Rourke model under predicts evaporation rate compared to Wittig.

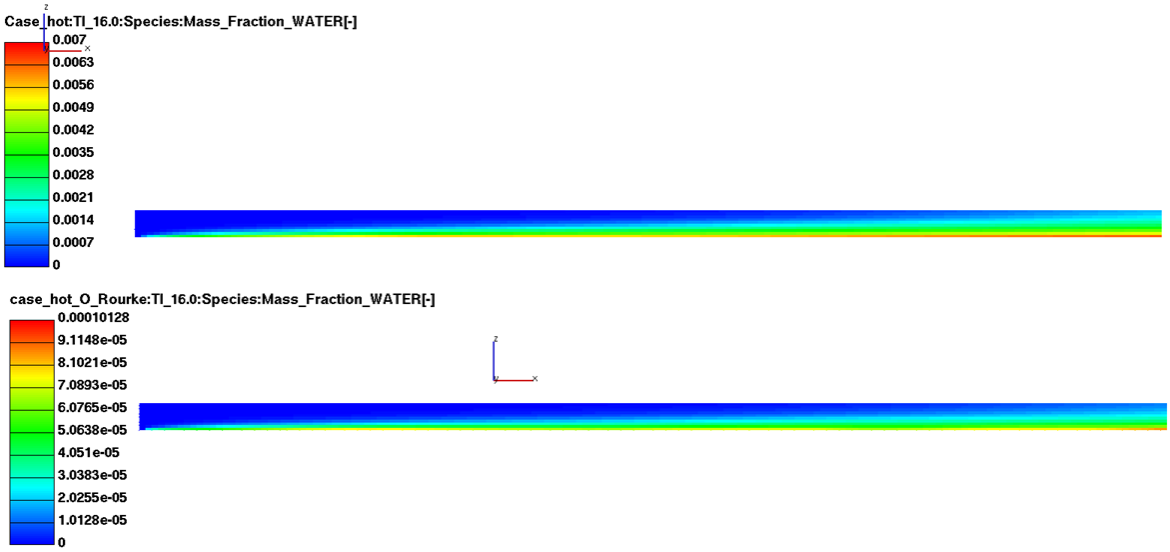


**Figure 3.** Qualitative comparison of water concentrations in the central cross section
**Slika 3.** Kvalitativna usporedba koncentracija vode na središnjem presjeku

In order to validate both models comparison with experimental data is presented. We can see that model on the basis of O'Rourke and Amsden under predicts concentrations compared to experiment, so that the agreement with data is not satisfactory. Reason behind this behaviour lays in the fact that wall functions for boundary layer above vaporizing films were derived without experimental back-up. It seems that physical reasoning behind them is at least qualitatively correct, but the model is not able to pick up experimental tests quantitatively.

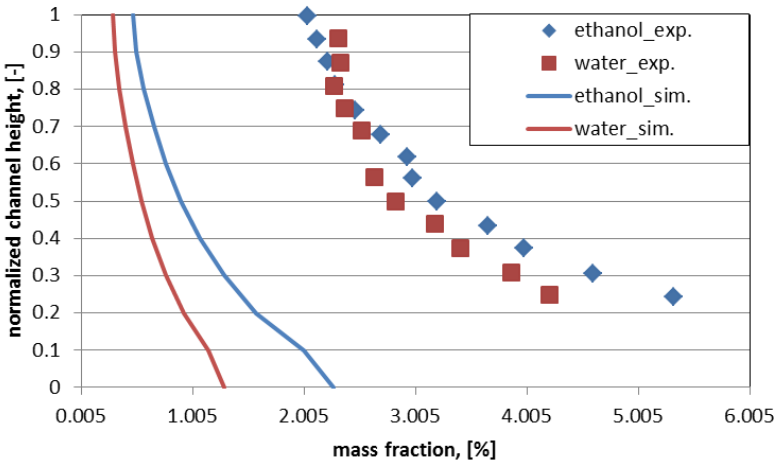


**Figure 4.** Comparison of gas phase concentrations in measurement plane 4 (O'Rourke model)
**Slika 4.** Kvalitativna usporedba koncentracija vode na središnjem presjeku

In the Figure 5 results of Wittig model show much better agreement with experiments. Here it should be noted that heat transfer in boundary layer was calculated with fixed Nusselt number, which was shown previously as a sound assumption in the case of the single component model. The validity of this model in single component case was generalized to multicomponent, and also employment of UNIFAC method has certain share in improved results. As a conclusion of this part, it can be said that Wittig's model should be employed due to better results. However, very limited experimental data on this topic makes it difficult to give definite conclusions. It should be noted that Figure 4 and Figure 5 represent high pressure conditions of 2.6 bar. There were also measurements carried out on the lower pressure of 1.1 bar in order to see what is the influence of pressure and whether newly developed model is able to capture those differences.

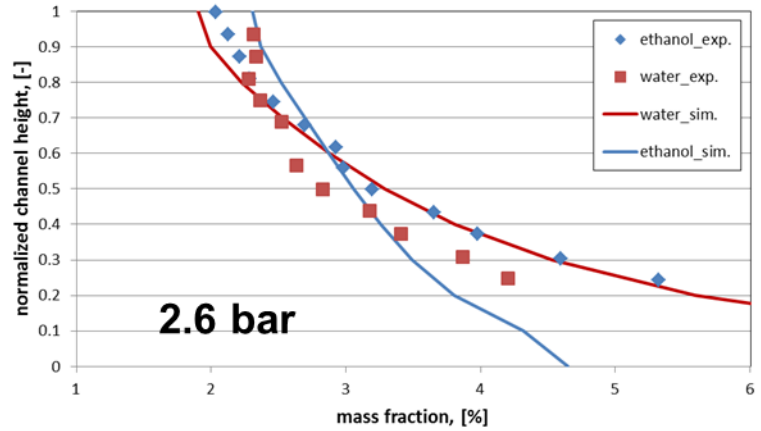


**Figure 5.** Comparison of gas phase concentrations in measurement plane 4 (Wittig model)
**Slika 5.** Usporedba koncentracija u plinskoj fazi u mjernoj ravnini br. 4 (O'Rourkeov model)

Comparison between Figure 5 and Figure 6 shows that lower pressure represents smaller resistance to evaporation, and consequently the concentrations in the gas phase of measurement plane 4 are higher. Since model based on the wall functions from O'Rourke and Amsden proved to be only qualitatively correct, comparison with experimental data on lower pressures was carried out only with Wittig model. It can be seen on Figure 6 that this model is able to capture experimental trend, especially in the case of ethanol concentrations. Agreement in the case of water concentrations is not so good, but still satisfactory, especially in the case of channel heights closer to the film surface. Moving away from the film surface, model under predicts water concentrations. One of the possible reasons for discrepancy from experimental results even in Wittig's model is using lumped parameter approach where physical quantities, such as film temperature and liquid mass fractions, are described as constant within film cell. Refinement of this assumption should entail employing of some polynomial function to better describe those quantities or discretization of film thickness. However, this would have negative impact on the computational requirements.

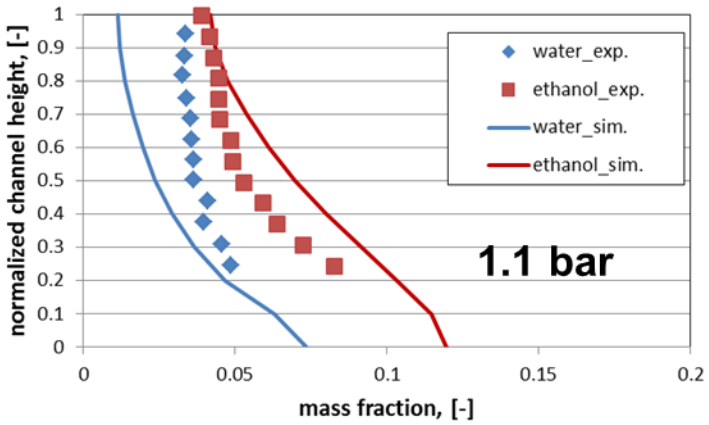


**Figure 6.** Comparison of gas phase concentrations in measurement plane 4 (Wittig model)
**Slika 6.** Usporedba koncentracija u plinskoj fazi u mjernoj ravnini br. 4 (Wittigov model)

Finally, Figure 7 enables better visualization of the influence of the gas phase pressure onto the evaporation dynamics. Great difference in the gas phase concentrations between different pressures can be observed. Using the same colour legend for both cases, higher pressure shows almost order of magnitude lower concentrations.

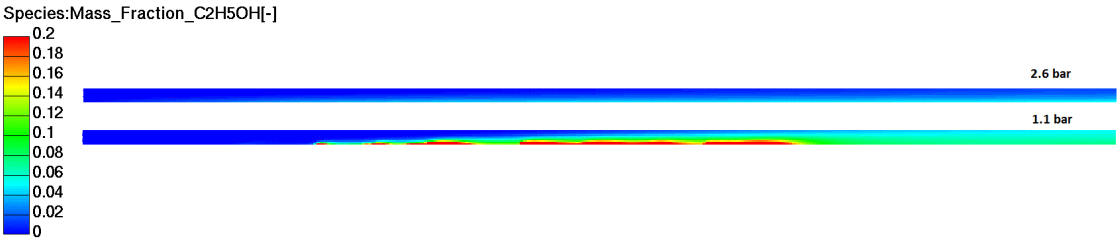


**Figure 7.** Influence of pressure on the gas phase concentrations - central cut
**Slika 7.** Utjecaj tlaka na koncentracije u plinskoj fazi – središnji presjek

## CONCLUSION

This work makes improvement of the Eulerian liquid wall film model through further development and implementation of numerical model of multicomponent evaporation, with the ultimate goal of achieving more accurate and computationally efficient calculations as a surrogate for experimental approaches.

Multicomponent evaporation has been modelled by two approaches, i.e. by employing modified wall functions derived by physical reasoning and utilizing the analogy between momentum and mass transfer. The latter approach showed more accurate in terms of comparison with experimental data from Wittig et al. [27]. However, very limited experimental data prevent for giving the definitive conclusion on this matter. The provisory nature of derived wall functions seems to be responsible for higher discrepancies from experiment. Particular scientific contribution presents implementation of UNIFAC method for activity coefficients calculation, which is employed in the area of liquid wall films for the first time. It enables more accurate calculation of interface concentrations in the case of multicomponent liquids which have a decisive influence on the evaporation rate.

Future work should include detailed modelling of liquid film properties, such as temperature and concentration, by employing some function dependency or film discretization procedure. It should be assessed how much would be that approach suitable by comparing increase in accuracy versus increase in computational time/resources.

**Acknowledgement**

*Financial support from the European Union's Horizon 2020 Phoenix Grant Agreement (NUMBER -690925 –Phoenix) is gratefully acknowledged.*

## REFERENCES

[1] Y. Ra, R.D. Reitz, Numerical Study of Multi-Component Spray Combustion with a Discrete Multi-Component Fuel Model, in: Int. Multidimens. Engine Model. User's Gr. Meet. SAE Congr., Detroit, 2009: p. 6.

[2] C.F. Lee, W.L. Cheng, D. Wang, Finite diffusion wall film evaporation model for engine simulations using continuous thermodynamics, Proc. Combust. Inst. 32 (2009) 2801–2808. doi:10.1016/j.proci.2008.06.087.

[3] P.J. O'Rourke, A.A. Amsden, A Particle Numerical Model for Wall Film Dynamics in Port-Injected Engines, 1996. doi:10.4271/961961.

[4] Y. Zeng, C. Lee, Multicomponent-Fuel Film-Vaporization Model for Multidimensional Computations, J. Propuls. Power. 16 (2000) 964–973. doi:10.2514/2.5697.

[5] D.J. Torres, P.J. O'rourke, A.A. Amsden, Efficient multicomponent fuel algorithm, Combust. Theory Model. 7 (2003) 66–86. doi:10.1088/1364-7830/7/1/304.

[6] Seyed Vahid Ebrahimian Shiadeh, Development of multi-component evaporation models and 3D modeling of NOx-SCR reduction system, Institut National Polytechnique de Toulouse, 2011.

[7] G. Desoutter, T.P. Habchi, Chawki, Bénédicte Cuenot, Single-component liquid film evaporation model development and validation using direct numerical simulations, in: Proc. ICLASS 2006, Kyoto, 2006: p. 8.

[8] X. Cui, X. Li, H. Sui, H. Li, Computational fluid dynamics simulations of direct contact heat and mass transfer of a multicomponent two-phase film flow in an inclined channel at sub-atmospheric pressure, Int. J. Heat Mass Transf. 55 (2012) 5808–5818. doi:10.1016/j.ijheatmasstransfer.2012.05.077.

[9] J.B. Haelssig, A.Y. Tremblay, J. Thibault, S.G. Etemad, Direct numerical simulation of interphase heat and mass transfer in multicomponent vapour–liquid flows, Int. J. Heat Mass Transf. 53 (2010) 3947–3960. doi:10.1016/j.ijheatmasstransfer.2010.05.013.

[10] S. Liye, Z. Weizheng, Z. Ti'en, Q. Zhaoju, A new approach to transient evaporating film heating modeling based on analytical temperature profiles for internal combustion engines, Int. J. Heat Mass Transf. 81 (2015) 465–469. doi:10.1016/j.ijheatmasstransfer.2014.10.061.

[11] Y. Yan, H. Liu, M. Jia, M. Xie, H. Yin, A one-dimensional unsteady wall film evaporation model, Int. J. Heat Mass Transf. 88 (2015) 138–148. doi:10.1016/j.ijheatmasstransfer.2015.04.082.

[12] G. Desoutter, Etude numérique de la propagation d'une flamme sous l'influence d'un film liquide de carburant sur la paroi, Institut National Polytechnique de Toulouse, 2007.

[13] D.W. Stanton, C.J. Rutland, Multi-dimensional modeling of thin liquid films and spray-wall interactions resulting from impinging sprays, Int. J. Heat Mass Transf. 41 (1998) 3037–3054. doi:10.1016/S0017-9310(98)00054-4.

[14] C. Bai, A.D. Gosman, Mathematical Modelling of Wall Films Formed by Impinging Sprays, 1996. doi:10.4271/960626.

[15] H. Foucart, C. Habchi, J.F. Le Coz, T. Baritaud, Development of a Three Dimensional Model of Wall Fuel Liquid Film for Internal Combustion Engines, 1998. doi:10.4271/980133.

[16] J. Ebner, P. Schober, O. Schäfer, S. Wittig, Modelling of Shear-Driven Liquid Wall Films on Curved Surfaces : Effect of Accelerated Air Flow and Variable Film Load, in: Proc. ICLASS 2003, 9th Trienn. Int. Conf. Liq. At. Spray Syst., Sorento, 2003.

[17] T. Lucchini, G. D'Errico, F. Brusiani, G.M. Bianchi, Ž. Tuković, H. Jasak, Multi-dimensional modeling of the air/fuel mixture formation process in a PFI engine for motorcycle applications, in: 2009. doi:10.4271/2009-24-0015.

[18] G. Cazzoli, C. Forte, Development of a model for the wall film formed by impinging spray based on a fully explicit integration method, (2005). doi:10.4271/2005-24-087.

[19] AVL, FIRE ® VERSION 2014.2 manual, (2015).

[20] E. Burck, Der Einfluß der Prandtl-Zahl auf den Wärmeuübergang und Druckverlust künstlich aufgerauhter Strömungskanäle, Wärme-Stoffübertrag. 2 (1969) 87–98.

[21] K.H. Sill, Wärme- und Stoffübergang in turbulenten Strömungsgrenz-schichten längs verdunstender welliger Wasserfilme, Karlsruhe Institute of Technology, 1982.

[22] C.L.V. Jayatilleke, The Influence of Prandtl Number and Surface Roughness on the Resistance of the Laminar Sub-Layer to Momentum and Heat Transfer, Prog. Heat Mass Transf. 1 (1969).

[23] B.E. Launder, D.B. Spalding, The numerical computation of turbulent flows, Comput. Methods Appl. Mech. Eng. 3 (1974) 269–289. doi:10.1016/0045-7825(74)90029-2.

[24] A. Fredenslund, P.R. J. Gmehling, Vapor-liquid Equilibria Using Unifac, Elsevier, Amsterdam, 1977. http://linkinghub.elsevier.com/retrieve/pii/B9780444416216500016.

[25] F. Brenn, G., Deviprasath, L.J. and Durst, Computations and Experiments on the Evaporation of Multi-Component Droplets, in: Proc.9th Int.Conf.Liquid At. Syst. (ICLASS), Sorento, 2003.

[26] S. Wittig, J. Himmelsbach, B. Noll, H.J. Feld, W. Samenfink, Motion and Evaporation of Shear-Driven Liquid Films in Turbulent Gases, J. Eng. Gas Turbines Power. 114 (1992) 395. doi:10.1115/1.2906604.

[27] M. Gerendas, S. Wittig, Experimental and Numerical Investigation on the Evaporation of Shear-Driven Multicomponent Liquid Wall Films, J. Eng. Gas Turbines Power. 123 (2001) 580. doi:10.1115/1.1362663.